complexities can be introduced by this fact, since it is not always clear which deformation map should be trusted. For example, deformation densities near Ti- and O-ion sites are rather different depending on the structural model subtracted. It is also not clear from these deformation maps which Ti—O bond is stronger, the two long apical bonds or the four short equatorial bonds, since deformation densities of two bonds were reversed depending on the model. It cannot be avoided that the information obtained from deformation maps is somewhat indirect compared with that of an MEM map.

7. Concluding remarks

The electron-density distribution in TiO_2 (rutile) has been obtained from X-ray powder diffraction data by analyzing the UDIS-MEM. The MEM map reveals not only the basic rutile structure but also a three-dimensional network structure consisting of TiO_2 'molecules'. It also demonstrated the skewness of the oxygen core electron-density distribution, which may be affected by the atomic polarization of oxygen. The present work again proved that the UDIS-MEM is a very powerful method for visualizing the details of the electron-density distribution. In order to interpret the 'observed' electron density, however, an analysis of both X-ray and neutron diffraction data for the same material is required. Such a study would provide a concrete answer as to whether the deformation of the electron density results from the lattice or the electron system. Through such studies, new aspects of crystallography may be developed.

The authors thank the Computer Center, Institute for Molecular Science, Okazaki National Research Institutes, for the use of the HITAC M-680H and S-820/80 computers and the library program *ABCXYZ* written by T. Yamada (IMS). A part of the computations in this work were also carried out at the Computer Center of Nagoya University which is gratefully acknowledged by the authors. This work has been partly supported by a Grant-in-Aid for Scientific Research from the Ministry of Education, Science and Culture.

References

Abrahams, S. C. & Bernstein, J. L. (1971). *J. Chem. Phys.* **55**, 3206–3211.
Baur, W. H. (1961). *Acta Cryst.* **14**, 209–213.
Bertaut, E. F. (1978). *J. Phys. (Paris)*, **39**, 1331–1347.
Collins, D. M. (1982). *Nature (London)*, **298**, 49–51.
Grants, F. A. (1959). *Rev. Mod. Phys.* **31**, 646–674.
Gronschorek, W. (1982). *Z. Kristallogr.* **160**, 187–203.
Gull, S. F. & Daniel, G. J. (1978). *Nature (London)*, **272**, 686–690.
Howard, C. J., Sabine, T. M. & Dickson, F. (1991). *Acta Cryst.* B**47**, 462–468.
Kingsbury, P. I. (1968). *Acta Cryst.* A**24**, 578–579.
Ladd, M. F. C. (1969). *Acta Cryst.* A**25**, 486–487.
Parker, R. A. (1961). *Phys. Rev.* **124**, 1719–1722.
Restori, R., Schwarzenbach, D. & Schneider, J. R. (1987). *Acta Cryst.* B**43**, 251–257.
Saka, T. & Kato, N. (1986). *Acta Cryst.* A**42**, 469–478.
Sakata, M., Mori, R., Kumazawa, S., Takata, M. & Toraya, H. (1990). *J. Appl. Cryst.* **23**, 526–534.
Sakata, M. & Sato, M. (1990). *Acta Cryst.* A**46**, 263–270.
Sen, S. K., Riga, J. & Verbist, J. (1976). *Chem. Phys. Lett.* **39**, 560–564.
Shintani, H., Sato, S. & Saito, Y. (1975). *Acta Cryst.* B**31**, 1981–1982.
Toraya, H. (1986). *J. Appl. Cryst.* **19**, 440–447.

Acta Cryst. (1992). B**48**, 598–604

Structures and Electron Density Distributions of $[Cl{-}P(NPCl_3)_3]^+.Cl^-$ and $[Cl{-}P(NPCl_3)_3]^+.PCl_6^-.\frac{1}{2}C_2H_2Cl_4$ at 100 K

By Ferdinand Belaj

Institut für Anorganische Chemie der Karl-Franzens-Universität Graz, Schubertstraße 1, A-8010 Graz, Austria

(*Received* 27 *November* 1991; *accepted* 26 *March* 1992)

Abstract

Chlorotris(trichlorophosphazeno)phosphonium chloride (1), $Cl_{11}N_3P_4$, $M_r = 555.9$, trigonal, $R3$, $a = 10.600$ (1), $c = 14.167$ (2) Å, $V = 1378.5$ (3) Å^3, $Z = 3$, $D_x = 2.009$ Mg m^{-3}, λ(Mo $K\alpha$) = 0.71069 Å, $\mu = 2.00$ mm^{-1}, $F(000) = 804$, $T = 100$ K, $R = 3.10$, $wR = 2.91$% for 1981 unique observed reflections and 54 parameters. Chlorotris(trichlorophosphazeno)phosphonium hexachlorophosphate–1,1,2,2-tetrachloroethane (2/1) (2), $Cl_{16}N_3P_5.\frac{1}{2}C_2H_2Cl_4$, $M_r = 848.1$, orthorhombic, $Cmca$, $a = 21.627$ (7), $b = 16.106$ (3), $c = 14.899$ (2) Å, $V = 5189.7$ (8) Å^3, $Z = 8$, $D_x = 2.171$ Mg m^{-3}, λ(Mo $K\alpha$) = 0.71069 Å, $\mu =$

0108-7681/92/050598-07$06.00

$2.22\ mm^{-1}$, $F(000) = 3272$, $T = 100$ K, $R = 2.41$, $wR = 2.29\%$ for 3223 unique observed reflections and 136 parameters. In these two ionic compounds the cations have site symmetries of 3 (1) and m (2). The P—N bonds to the central P atom are only slightly longer, and the P—N bonds of the $NPCl_3$ groups distinctly shorter than the P—N bonds observed in $(NPCl_2)_3$. Whereas the $NPCl_3$ group of (2), lying beside the mirror plane, resembles the $NPCl_3$ group of (1), the other $NPCl_3$ group of (2), lying in the mirror plane, shows a substantially larger P—N—P angle [157.2 (2) compared to 138.8 (1) or 134.8 (2)° in (1)] and quite different torsion angles. Despite these geometry variations, the deformation density maps show similar features.

Introduction

The present study is the first in a series of studies on phosphonitrile structures. Whereas crystallographic data are available for some cyclic $(X_2PN)_n$ compounds, the structures of open-chained trichlorophosphonitriles are unknown except for a few examples determined at room temperature: $[Cl_3PNPCl_3]X$ with $X^- = MoCl_6^-$, $MoOCl_4^-$ (Müller, Conradi, Patt-Siebel, Kersting, Schmidt, Khabou & Dehnicke, 1988) and $X^- = PCl_6^-$ (Faggiani, Gillespie, Sawyer & Tyrer, 1980), $[C(NPCl_3)_3]SbCl_6$ (Müller, 1980), $[C\{NP(Br_{0.78}Cl_{0.22})_3\}_3]SbBr_6$ (Müller & Schmock, 1980), $(Cl_3C)_2C(Cl)NPCl_3$ (Antipin, Struchkov, Yurchenko & Kozlov, 1982), and $(F_3C)_3CNPCl_3$ (Antipin, Struchkov & Kozlov, 1985).

Kirsanov reaction of $SP(NH_2)_3$ with PCl_5 in *sym*-$C_2H_2Cl_4$ gives colourless crystals of $[Cl—P(NPCl_3)_3]^+.Cl^-$ (1) (Becke-Goehring, Mann & Euler, 1961) or light-yellow crystals of $[Cl—P(NPCl_3)_3]^+.PCl_6^-.\frac{1}{2}C_2H_2Cl_4$ (2) (Latscha, Haubold & Becke-Goehring, 1965) depending on the ratio of the reagents. Compound (1) can also be obtained by reaction of $OP(NHSiMe_3)_3$ with PCl_5 in *sym*-$C_2H_2Cl_4$ (Riesel & Täschner, 1980). ^{31}P NMR and conductivity measurements have established the ionic nature of compounds (1) and (2) (Latscha, Haubold & Becke-Goehring, 1965). In order to study the electron density distribution, all measurements were carried out at low temperature. Because of the absence of elements lighter than nitrogen [disregarding the solvent molecule in (2)], which results in more precise atomic parameters, and because of the absence of elements heavier than chlorine, which prevents core-electron density dominating too much over valence-electron density, the trichlorophosphonitriles should be well suited to such a study. The different crystallographic site symmetries of the cation in (1) and (2) provides an internal check on the consistency of the results.

Experimental

Single crystals of (1) and (2) obtained by Kirsanov reactions of $SP(NH_2)_3$ with PCl_5 in *sym*-$C_2H_2Cl_4$ were immersed in oil and immediately cooled to 100 K. The crystal data and some details of the experimental conditions and of the refinements are given in Table 1. The X-ray measurements were performed on a modified Stoe four-circle diffractometer with graphite monochromator and a Nonius low-temperature device. Data corrections for Lorentz and polarization effects; structure solutions by direct methods; empirical absorption corrections with *DIFABS* (Walker & Stuart, 1983); full-matrix least-squares refinements (on F) with anisotropic thermal parameters for all non-H atoms and isotropic thermal parameters for the H atoms (C—H distance constrained to 1.08 Å) of the solvent molecules in (2) until $\Delta/\sigma \leq 0.002$; function $\sum w(|F_o| - |F_c|)^2$ minimized with $w = 1/\sigma^2(F_o)$. Additional high-order refinements were carried out (see Table 1) and the positional and thermal parameters obtained were used to calculate the $X—X$ deformation maps. Neutral atomic scattering factors and anomalous-dispersion corrections were taken from *International Tables for X-ray Crystallography* (1974, Vol. IV, pp. 99, 149). VAX/VMS 6000 computer, programs used: *SHELX76* (Sheldrick, 1976), *SHELXS86* (Sheldrick, 1986), *PLATON* (Spek, 1982), *ORTEP* (Johnson, 1965), *DFP* (Belaj, 1989), *NORM* (Belaj, 1992).

Results and discussion

The final atomic positional and thermal parameters for compounds (1) and (2) are given in Table 2,* the bond lengths and angles in Tables 3 and 4, respectively. Atomic labelling is shown in Figs. 1 and 2.

The structure analyses confirm the ionic nature of the compounds. In (1), the cations and anions lie on threefold rotation axes. In (2), the cation, the anion and the solvent molecule have m, $\bar{1}$ and $2/m$ symmetry, respectively. Comparison of the geometry of the cations in the two compounds shows mainly the following (see Fig. 3): the $NPCl_3$ group of the cation of compound (2) lying beside the mirror plane resembles the $NPCl_3$ group of the cation of compound (1), which does not even approximately show $3m$ symmetry, even for the Cl(1)—P(1)—N—P and P(1)—N—P—Cl torsion angles, whereas the $NPCl_3$ group of (2) lying in the mirror plane shows a

* Lists of anisotropic thermal parameters and structure factors, and difference electron density maps showing sections through the PCl_6^- ion have been deposited with the British Library Document Supply Centre as Supplementary Publication No. SUP 55115 (15 pp.). Copies may be obtained through The Technical Editor, International Union of Crystallography, 5 Abbey Square, Chester CH1 2HU, England. [CIF reference: SE0086]

Table 1. *Experimental crystal data, data collection and refinement data for* (1) *and* (2)

	(1)	(2)
Crystal size (mm)	0.32 × 0.35 × 0.45	0.25 × 0.35 × 0.40
Reflections used for cell refinement	93	100
2θ range for cell parameter determination (°)	13–28	10–23
Transmission range	0.835–1.153	0.748–1.011
$2\theta_{max}$ (°)	70	60
hkl range *h*	−17–17	−22–22
k	−17–17	−30–30
l	0–22	0–20
Scan type and range (°)	ω–2θ; 2.0	ω; 1.5
Maximum intensity variation of standard reflections (%)	± 1.44	± 2.58
No. of measurements	4199	13 080
No. of unique reflections	2239	4316
R_{int}	0.0215	0.0276
Least-squares refinement (all data)		
Observed data with $I > 3\sigma(I)$	1981	3233
No. of excluded reflections (weakened by extinction)	0	10
No. of parameters	54	136
$R = \sum\lvert\lvert F_o\rvert - \lvert F_c\rvert\rvert/\sum\lvert F_o\rvert$	0.0310	0.0241
$wR = \sum w^{1/2}(\lvert F_o\rvert - \lvert F_c\rvert)/\sum w^{1/2}\lvert F_o\rvert$	0.0291	0.0229
$S = [\sum w(\lvert F_o\rvert - \lvert F_c\rvert)^2/(N_{ref} - N_{par})]^{1/2}$	2.10	1.54
Maximum height in difference map (e Å^{-3})	0.618	0.574
Least-squares refinement (high-order data)		
Limit of $\sin\theta/\lambda$ (Å^{-1})	0.60	0.55
Observed data with $I > 3\sigma(I)$	1355	1620
No. of parameters	54	136
$R = \sum\lvert\lvert F_o\rvert - \lvert F_c\rvert\rvert/\sum\lvert F_o\rvert$	0.0382	0.0305
$wR = \sum w^{1/2}(\lvert F_o\rvert - \lvert F_c\rvert)/\sum w^{1/2}\lvert F_o\rvert$	0.0357	0.0255
$S = [\sum w(\lvert F_o\rvert - \lvert F_c\rvert)^2/(N_{ref} - N_{par})]^{1/2}$	1.63	1.28
Maximum height in difference map (e Å^{-3})	0.231	0.297

Table 2. *Fractional atomic coordinates* ($\times 10^5$) *and equivalent isotropic thermal parameters* (Å$^2 \times 10^4$) *for* (1) *and* (2) *with e.s.d.'s in parentheses*

$U_{eq} = \frac{1}{3}$ trace **U**.

	x	*y*	*z*	U_{eq}
(1)				
Cl(1)	0	0	76696 (10)	211 (4)
P(1)	0	0	62536 (10)	128 (4)
N(1)	16102 (21)	5347 (22)	58924 (17)	156 (10)
P(2)	31157 (6)	18861 (6)	60756 (8)	141 (3)
Cl(2)	44498 (6)	21421 (7)	50370 (8)	218 (3)
Cl(3)	31640 (7)	37589 (7)	62086 (9)	227 (3)
Cl(4)	40843 (8)	17343 (8)	72341 (9)	261 (4)
Cl(5)	0	0	0	165 (4)
(2)				
P(1)	0	6284 (4)	78900 (4)	117 (3)
Cl(1)	0	8215 (5)	92181 (4)	273 (4)
N(2)	0	15074 (13)	74265 (15)	183 (10)
P(2)	0	24383 (4)	73698 (4)	146 (3)
Cl(21)	0	30160 (5)	85259 (5)	420 (5)
Cl(22)	7176 (3)	28697 (3)	67176 (5)	428 (3)
N(3)	5831 (7)	900 (9)	76282 (11)	176 (7)
P(3)	12892 (2)	1266 (3)	77172 (3)	134 (2)
Cl(31)	15981 (2)	−2779 (3)	88769 (3)	245 (2)
Cl(32)	16672 (2)	12214 (3)	75565 (3)	236 (2)
Cl(33)	16717 (2)	−5955 (3)	68195 (4)	270 (3)
P(4)	25000	25000	100000	118 (3)
Cl(41)	26374 (2)	27592 (3)	86079 (3)	161 (2)
Cl(42)	15435 (2)	22455 (3)	97426 (3)	192 (2)
Cl(43)	27194 (2)	12264 (3)	97664 (3)	172 (2)
C(5)	0	46978 (15)	3900 (16)	142 (11)
H(5)	0	49752 (192)	10498 (95)	319 (92)
Cl(5)	6705 (2)	40664 (3)	3350 (3)	213 (2)

Table 3. *Bond distances* (Å), *bond angles* (°) *and torsion angles* (°) *for* (1)

Cl(1)—P(1)	2.006 (2)	Cl(4)—P(2)	1.985 (2)
Cl(2)—P(2)	1.963 (1)	P(1)—N(1)	1.590 (3)
Cl(3)—P(2)	1.969 (1)	P(2)—N(1)	1.543 (2)
Cl(1)—P(1)—N(1)	108.8 (1)	Cl(2)—P(2)—Cl(3)	106.17 (5)
N(1)—P(1)—N(1^i)	110.2 (1)	Cl(2)—P(2)—Cl(4)	105.36 (5)
N(1)—P(2)—Cl(2)	110.0 (1)	Cl(3)—P(2)—Cl(4)	104.41 (6)
N(1)—P(2)—Cl(3)	116.5 (1)	P(1)—N(1)—P(2)	134.8 (2)
N(1)—P(2)—Cl(4)	113.6 (1)		

Cl(1)—P(1)—N(1)—P(2)	−54.0 (2)
N(1^i)—P(1)—N(1)—P(2)	65.1 (3)
N(1^{ii})—P(1)—N(1)—P(2)	−173.1 (2)
Cl(2)—P(2)—N(1)—P(1)	−158.4 (2)
Cl(3)—P(2)—N(1)—P(1)	−37.7 (3)
Cl(4)—P(2)—N(1)—P(1)	83.8 (2)

Symmetry code: (i) $-y, x-y, z$; (ii) $y-x, -x, z$.

Table 4. *Bond distances* (Å), *bond angles* (°) *and torsion angles* (°) *for* (2)

Cl(1)—P(1)	2.003 (1)	P(2)—N(2)	1.502 (2)
Cl(21)—P(2)	1.958 (1)	P(3)—N(3)	1.534 (2)
Cl(22)—P(2)	1.959 (1)	Cl(5)—C(5)	1.773 (2)
Cl(31)—P(3)	1.9637 (9)	C(5)—C(5^{iii})	1.516 (3)
Cl(32)—P(3)	1.9583 (9)	C(5)—H(5)	1.08
Cl(33)—P(3)	1.9560 (9)	Cl(41)—P(4)	2.1365 (8)
P(1)—N(2)	1.575 (2)	Cl(42)—P(4)	2.1434 (8)
P(1)—N(3)	1.579 (2)	Cl(43)—P(4)	2.1340 (8)
Cl(1)—P(1)—N(2)	107.07 (9)	Cl(5)—C(5)—Cl(5^i)	109.7 (1)
Cl(1)—P(1)—N(3)	109.22 (7)	Cl(5)—C(5)—C(5^{iii})	109.4 (1)
N(2)—P(1)—N(3)	112.66 (7)	Cl(5)—C(5)—H(5)	106.2 (8)
N(3)—P(1)—N(3^i)	105.97 (8)	C(5^{iii})—C(5)—H(5)	116 (1)
Cl(21)—P(2)—Cl(22)	105.54 (3)	Cl(41)—P(4)—Cl(42)	89.88 (2)
Cl(21)—P(2)—N(2)	115.15 (9)	Cl(41)—P(4)—Cl(43)	89.92 (2)
Cl(22)—P(2)—N(2)	112.47 (5)	Cl(41)—P(4)—Cl(41^{ii})	180
Cl(22)—P(2)—Cl(22^i)	104.83 (4)	Cl(41)—P(4)—Cl(42^{ii})	90.12 (2)
Cl(31)—P(3)—Cl(32)	105.32 (3)	Cl(41)—P(4)—Cl(43^{ii})	90.08 (2)
Cl(31)—P(3)—Cl(33)	105.10 (3)	Cl(42)—P(4)—Cl(43)	90.09 (2)
Cl(31)—P(3)—N(3)	113.70 (7)	Cl(42)—P(4)—Cl(41^{ii})	90.12 (2)
Cl(32)—P(3)—Cl(33)	105.98 (3)	Cl(42)—P(4)—Cl(42^{ii})	180
Cl(32)—P(3)—N(3)	116.08 (6)	Cl(42)—P(4)—Cl(43^{ii})	89.91 (2)
Cl(33)—P(3)—N(3)	109.82 (6)	Cl(43)—P(4)—Cl(41^{ii})	90.08 (2)
P(1)—N(2)—P(2)	157.2 (2)	Cl(43)—P(4)—Cl(42^{ii})	89.91 (2)
P(1)—N(3)—P(3)	138.8 (1)	Cl(43)—P(4)—Cl(43^{ii})	180

Cl(1)—P(1)—N(2)—P(2)	0
N(3)—P(1)—N(2)—P(2)	−120.09 (7)
Cl(1)—P(1)—N(3)—P(3)	−57.0 (2)
N(2)—P(1)—N(3)—P(3)	61.9 (2)
N(3^i)—P(1)—N(3)—P(3)	−174.5 (2)
Cl(21)—P(2)—N(2)—P(1)	0
Cl(22)—P(2)—N(2)—P(1)	120.96 (4)
Cl(31)—P(3)—N(3)—P(1)	83.7 (2)
Cl(32)—P(3)—N(3)—P(1)	−38.7 (2)
Cl(33)—P(3)—N(3)—P(1)	−158.9 (1)
Cl(5)—C(5)—C(5^{iii})—Cl(5^{iv})	59.7 (2)
Cl(5)—C(5)—C(5^{iii})—Cl(5^{iii})	180
Cl(5)—C(5)—C(5^{iii})—H(5^{iii})	−60.2 (1)
H(5)—C(5)—C(5^{iii})—H(5^{iii})	180

Symmetry code: (i) $-x, y, z$; (ii) $\frac{1}{2}-x, \frac{1}{2}-y, 2-z$; (iii) $-x, 1-y, 2-z$; (iv) $x, 1-y, 2-z$.

substantially larger P—N—P angle [157.2 (2) compared to 138.8 (1) or to 134.8 (2)° in (1)] and quite different torsion angles. Nevertheless, the two cations show approximately *cisoid* configurations about their Cl(1)—P(1)···P—Cl torsion angles

[24.49 (4)° in (1), 22.42 (4) and 0° in (2)], as observed in $[Cl_3PNPCl_3][PCl_6]$ (Faggiani, Gillespie, Sawyer & Tyrer, 1980). The P(1)—N bonds are only slightly longer, and the P—N bonds of the $NPCl_3$ groups distinctly shorter than the value of 1.575 (3) Å observed in $(NPCl_2)_3$ (Bullen, 1971). Therefore, the P—N bond lengths suggest multiple-bond character for both the P(1)—N bonds and to a greater degree for the other P—N bonds according to the mesomerism

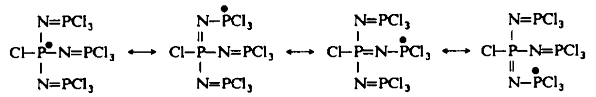

As found from ^{31}P NMR data (Latscha, Haubold & Becke-Goehring, 1965), the first contributing form is of less importance: in both cations, the Cl(1)—P(1) bond is significantly longer than the P—Cl bonds of the $NPCl_3$ groups.

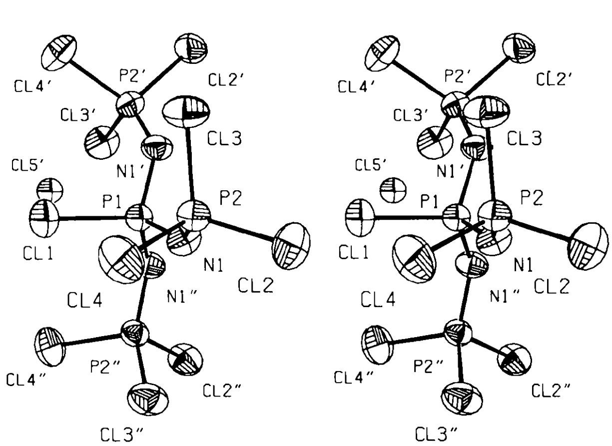

Fig. 1. *ORTEP* stereo plot showing the numbering scheme of (1) (symmetry codes as defined in Table 3). Thermal ellipsoids are drawn at the 90% probability level.

The structure of the $[Cl—P(NPCl_3)_3]^+$ cation at the semi-empirical MNDO/PM3 level (modified neglect of diatomic overlap/parametric method 3) (Stewart, 1989*a*,*b*) was calculated and the local energy minimum confirmed by the calculated complete set of harmonic vibrational frequencies gave quite different geometric parameters: P—N—P angles of 169.8°, P—Cl bond lengths 2.015–2.022 Å, P—N bond lengths to the central P atom 1.654 Å, to the other P atoms 1.536 Å. Atomic charges were: −0.31 (Cl), +2.28 (central P), +1.91 (other P), −1.29 (N).

The packings of compounds (1) and (2) in the unit cell are shown in Figs. 4 and 5, respectively. The Cl^- ions in (1) have a coordination number of 7 [3 × Cl(3), 3 × Cl(2), 1 × Cl(1) with distances to Cl(5) of 3.066 (1), 3.158 (1) and 3.302 (1) Å, respectively; no other distances below 5 Å]. The coordination polyhedron (C_3 symmetry) shows a geometry between a monocapped octahedron and a trigonal prism with one monocapped triangle (both C_{3v} symmetry): the mutual rotation angle between the Cl(1)—Cl(5)—Cl(2) plane and the Cl(1)—Cl(5)—Cl(3) plane is 24.56 (5)° (60°/0° for the octahedral/prismatic arrangement). As expected, the PCl_6^- anion in (2) shows even larger bond lengths than the P—Cl bonds of the $NPCl_3$ groups and forms an almost perfect octahedron. The PCl_6^- ion, where the negative charge is more dispersed over the anion compared to the Cl^- ion in (1), is surrounded by many Cl atoms at greater distances: 12 Cl···Cl contacts 3.354 (1)–3.517 (1) Å, 14 further contacts 3.590 (1)–3.706 (1) Å [next distance 3.991 (1) Å]. The $C_2H_2Cl_4$ molecules have staggered *anti* conformations and occupy the holes in the framework built up by the ions; no disorder could be detected.

Deformation electron density maps representing the difference between the actual observed electron

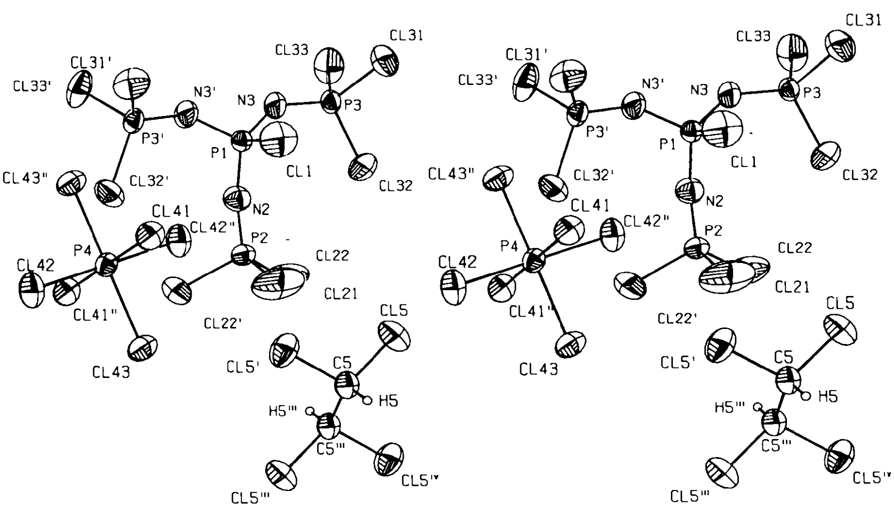

Fig. 2. *ORTEP* stereo plot showing the numbering scheme of (2) (symmetry codes as defined in Table 4). Thermal ellipsoids are drawn at the 90% probability level, the H atoms with an arbitrary radius.

density and the superposition of spherically averaged free-atom densities allowed for anisotropic thermal vibration were calculated in several sections for both compounds. The atomic parameters resulting from the high-order refinements show only small differences from those resulting from the refinements with the full data set. With normal and half-normal probability plots (Abrahams & Keve, 1971) the experimental differences in parameters relative to the combined standard deviations of the parameters, arranged in order of increasing magnitude, were compared with the values expected for normal distributions: half-normal probability plots (deposited) of x, y, z, U_{13}, U_{23} and of U_{12} [U_{12} only for compound (2)] for the non-H atoms have zero intercepts and slopes close to unity indicating realistic standard deviations and the presence of only random errors in these parameters. By contrast, the normal probability plots (see Fig. 6) of U_{11}, U_{22}, U_{33} and of U_{12} [only for (1), where U_{12} is symmetry-correlated to U_{11} and U_{22}] have, especially for the noncentrosymmetric compound (1), negative intercepts denoting a systematic increase of the U_{ii} and U_{12} parameters in the high-order parameter set of (1) of about twice the combined standard deviations.

Since the deformation density is very sensitive to systematic errors, the reliability of the maps was checked in two ways: according to the 'rigid-bond' postulate (Hirshfeld, 1976), the difference $|z^2_{A,B} - z^2_{B,A}|$ should be less than about 0.001 Å^2 for every covalently bonded pair of atoms A and B, where $z^2_{A,B}$ denotes the mean-square amplitude of vibration of the atom A along the direction of the bond. Table 5 shows that this postulate is almost fulfilled: only the

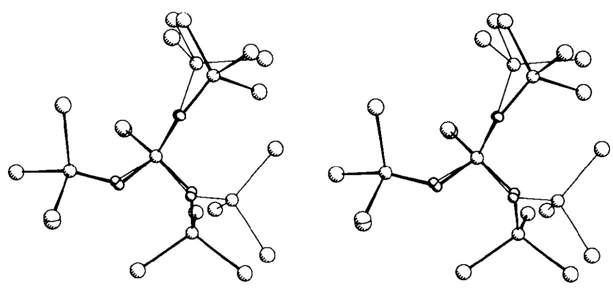

Fig. 3. Comparison of the conformations of the cations of (1) and (2): least-squares fit of the atomic positions of Cl(1), P(1) and of the $NPCl_3$ group lying beside the mirror plane [N(3), P(3), Cl(3x), x = 1–3] of (2) (thin lines) to the atomic positions of Cl(1), P(1) and one $NPCl_3$ group of (1) (thick lines).

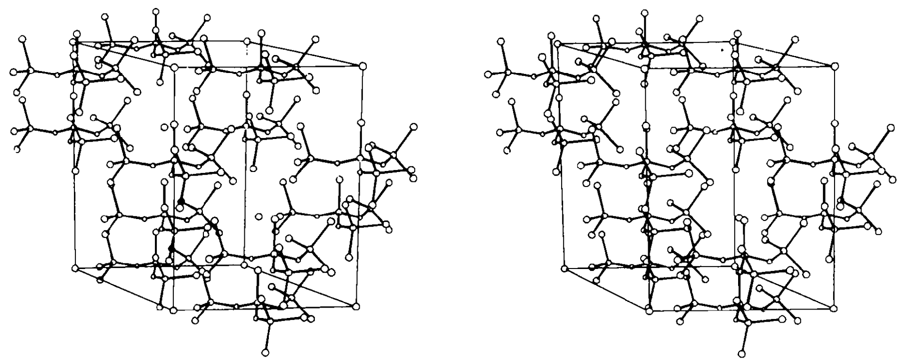

Fig. 4. Stereoscopic view of the packing in the crystal structure of (1). The atoms are drawn as spheres with arbitrary radii.

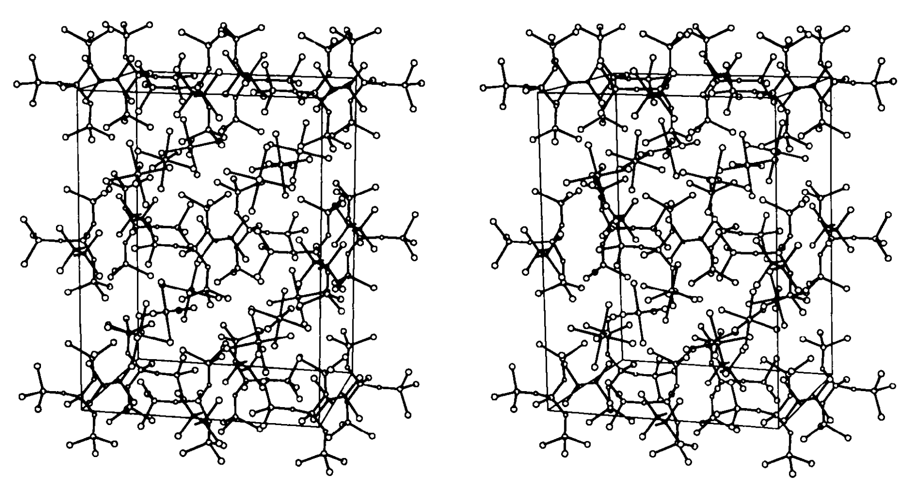

Fig. 5. Stereoscopic view of the packing in the crystal structure of (2). The atoms are drawn as spheres with arbitrary radii.

Table 5. *Mean-square vibrational amplitudes* ($Å^2 \times 10^4$) *of pairs of bonded atoms A and B in the direction of bond A—B for compounds* (1) (*above*) *and* (2) (*below*)

A	B	$z^2_{A,B}$	$z^2_{B,A}$	$z^2_{A,B} - z^2_{B,A}$
Cl(1)	P(1)	143 (4)	148 (4)	−5 (5)
Cl(2)	P(2)	165 (3)	166 (3)	−1 (5)
Cl(3)	P(2)	147 (4)	148 (3)	−1 (5)
Cl(4)	P(2)	146 (4)	142 (3)	4 (5)
P(1)	N(1)	124 (4)	136 (9)	−12 (10)
P(2)	N(1)	128 (3)	131 (9)	−3 (9)
Cl(1)	P(1)	135 (4)	127 (3)	8 (6)
Cl(21)	P(2)	137 (7)	141 (4)	−4 (8)
Cl(22)	P(2)	160 (5)	155 (4)	5 (6)
Cl(31)	P(3)	146 (3)	146 (3)	0 (4)
Cl(32)	P(3)	154 (3)	156 (3)	−2 (4)
Cl(33)	P(3)	133 (3)	133 (3)	0 (4)
P(1)	N(2)	112 (3)	119 (13)	−7 (13)
P(1)	N(3)	115 (3)	127 (8)	−12 (9)
P(2)	N(2)	110 (4)	130 (13)	−20 (13)
P(3)	N(3)	99 (3)	110 (8)	−11 (9)
Cl(41)	P(4)	110 (2)	111 (3)	−1 (4)
Cl(42)	P(4)	135 (3)	133 (3)	2 (4)
Cl(43)	P(4)	123 (3)	120 (3)	3 (4)
Cl(5)	C(5)	142 (3)	143 (12)	−1 (12)
C(5)	C(5^{iii})	142 (12)	142 (12)	0

Symmetry code: (iii) $-x$, $1-y$, $2-z$.

N atoms show vibrational amplitudes which are too large. The maximum difference $|z^2_{A,B} - z^2_{B,A}|$ of 0.0047 (11) $Å^2$ resulting from refinement with the full data set is reduced to 0.0020 (13) $Å^2$ using the high-order data. While the PCl_6^- ion and the $C_2H_2Cl_4$ molecules behave as rigid bodies [$|z^2_{A,B} - z^2_{B,A}| \leq$ 0.001 (1) $Å^2$ for non-bonded distances also], some internal torsional motions are observed in the cations leading to $|z^2_{A,B} - z^2_{B,A}|$ differences of up to 0.010 (1) and 0.026 (1) $Å^2$ for non-bonded distances in (1) and in (2), respectively.

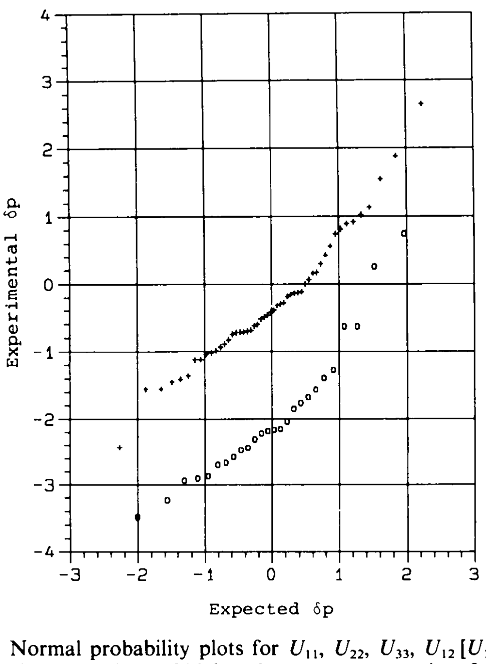

Fig. 6. Normal probability plots for U_{11}, U_{22}, U_{33}, U_{12} [U_{12} only for (1)]. Comparison of high-order parameters against full data parameters for (1) (o) and for (2) (+). $\delta p_{\rm experimental} = (p_{\rm full} - p_{\rm high})/[\sigma^2(p_{\rm full}) + \sigma^2(p_{\rm high})]^{1/2}$.

A second check was carried out for compound (2): three orthogonal sections through the central P atom P(4) and four Cl atoms of the PCl_6^- anion (deposited) show very similar features with deformation electron density maxima near the midpoints of the P—Cl bonds. The maps depicted were calculated

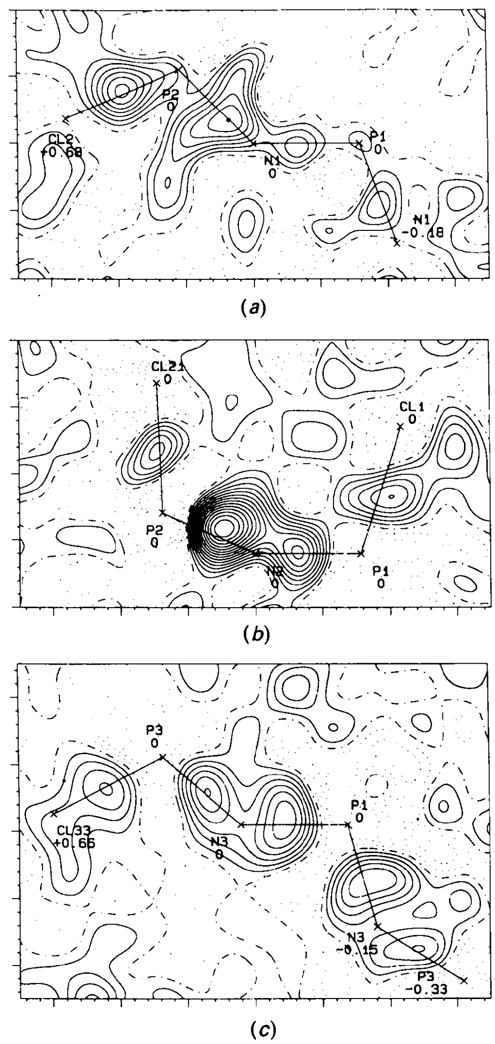

Fig. 7. Deformation electron density maps. Sections through (*a*) the cation in (1), (*b*) the N=PCl$_3$ group lying in the mirror plane in (2), (*c*) the N=PCl$_3$ group lying beside the mirror plane in (2). The average values for $\sigma(\Delta\rho)$ are 0.052, 0.096 and 0.068 e $Å^{-3}$, respectively. Contour interval 0.05 e $Å^{-3}$, negative contours dotted, zero contours chain-dotted. The numbers specify the site of the atoms above/below the sectional planes (in Å).

using only reflections with $\sin\theta/\lambda < 0.5$ Å^{-1}: the $P(NPCl_3)_3]^+$ cations obtained with data sets of increasing $\sin\theta/\lambda$ cut-offs revealed that above approximately 0.5 Å^{-1} the large number of weak reflections with relatively large experimental standard deviations leads to a disturbing increase in the noise level. The standard deviations (Coppens & Hamilton, 1968) do not include the errors of the scale factors and are larger near the atom centers (Stevens & Coppens, 1976). In compound (1) an additional phase error caused by the lack of a center of symmetry (Coppens, 1974) must be considered.

Despite the different crystallographic site symmetries of the cations in (1) and (2), the dynamic deformation density maps (see Fig. 7) show some common features: accumulation of negative charges between the atoms, charge transfer from the phosphorus to the more electronegative N atoms. Charge deficiency (positive charge) at the phosphorus atoms and higher charge densities along the P—N bonds than along the P—Cl single bonds were only observed in the deformation density maps of the centrosymmetric compound (2). Because of the mesomerism in the $[Cl—P(NPCl_3)_3]^+$ cations stated above and the small differences in the P—N bond distances, the charge densities along the P—N bonds of the $NPCl_3$ group are about the same or only slightly larger than the charge densities along the P—N bonds to the central phosphorus atom P(1).

The author thanks Dr Ch. Kratky, Institute of Physical Chemistry, University of Graz, for the use of the diffractometer.

References

Abrahams, S. C. & Keve, E. T. (1971). *Acta Cryst.* **A27**, 157–165.
Antipin, M. Yu., Struchkov, Yu. T. & Kozlov, E. S. (1985). *Zh. Strukt. Khim.* **26**, 96–102.
Antipin, M. Yu., Struchkov, Yu. T., Yurchenko, V. M. & Kozlov, E. S. (1982). *Zh. Strukt. Khim.* **23**, 72–76.
Becke-Goehring, M., Mann, T. & Euler, H. D. (1961). *Chem. Ber.* **94**, 193–198.
Belaj, F. (1989). *DFP*. Program for calculating and plotting difference Fourier density maps. Univ. of Graz, Austria.
Belaj, F. (1992). *NORM*. (Half-)normal probability plot program. Univ. of Graz, Austria.
Bullen, G. J. (1971). *J. Chem. Soc. A*, pp. 1450–1453.
Coppens, P. (1974). *Acta Cryst.* **B30**, 255–261.
Coppens, P. & Hamilton, W. C. (1968). *Acta Cryst.* **B24**, 925–929.
Faggiani, R., Gillespie, R. J., Sawyer, J. F. & Tyrer, J. D. (1980). *Acta Cryst.* **B36**, 1014–1017.
Hirshfeld, F. L. (1976). *Acta Cryst.* **A32**, 239–244.
Johnson, C. K. (1965). *ORTEP*. Report ORNL-3794. Oak Ridge National Laboratory, Tennessee, USA.
Latscha, H.-P., Haubold, W. & Becke-Goehring, M. (1965). *Z. Anorg. Allg. Chem.* **339**, 82–86.
Müller, U. (1980). *Z. Anorg. Allg. Chem.* **463**, 117–122.
Müller, U., Conradi, E., Patt-Siebel, U., Kersting, M., Schmidt, I., Khabou, A. & Dehnicke, K. (1988). *Z. Anorg. Allg. Chem.* **560**, 93–104.
Müller, U. & Schmock, F. (1980). *Z. Anorg. Allg. Chem.* **468**, 165–171.
Riesel, L. & Täschner, C. (1980). *Z. Anorg. Allg. Chem.* **465**, 120–126.
Sheldrick, G. M. (1976). *SHELX76*. Program for crystal structure determination. Univ. of Cambridge, England.
Sheldrick, G. M. (1986). *SHELXS86*. Program for the solution of crystal structures. Univ. of Göttingen, Germany.
Spek, A. L. (1982). *Computational Crystallography*, edited by D. Sayre, p. 528. Oxford: Clarendon Press.
Stevens, E. D. & Coppens, P. (1976). *Acta Cryst.* **A32**, 915–917.
Stewart, J. J. P. (1989*a*). *J. Comput. Chem.* **10**, 209–220.
Stewart, J. J. P. (1989*b*). *J. Comput. Chem.* **10**, 221–264.
Walker, N. & Stuart, D. (1983). *Acta Cryst.* **A39**, 158–166.

Acta Cryst. (1992). **B48**, 604–609

Structural Features of γ-Phase Bi_2O_3 and its Place in the Sillenite Family

By S. F. Radaev and V. I. Simonov

Institute of Crystallography, Russian Academy of Sciences, Leninsky pr. 59, 117333 *Moscow, Russia*

and Yu. F. Kargin

Institute of General and Inorganic Chemistry, Russian Academy of Sciences, Leninsky pr. 31, 117071 *Moscow, Russia*

(*Received* 1 *August* 1991; *accepted* 6 *April* 1992)

Abstract

A new atomic model of the γ-phase of bismuth trioxide, Bi_2O_3, has been suggested, explained and refined from powder neutron diffraction data. The data were collected at 293 K. $Bi_{12}Bi_{0.80}O_{19.20}$, M_r = 2982.1, cubic, $I23$, a = 10.2501 (5) Å, V = 1076.9 (2) Å^3, Z = 2, D_m = 9.18, D_x = 9.20 g cm^{-3}, λ = 2.3145 Å, μ = 0.0008 cm^{-1}, R_{wp} = 6.56% for 1206 profile points. It was found that the tetrahedral sites

0108-7681/92/050604-06$06.00